Adhesive contact of cylindrical lens and a flat sheet

Manoj K. Chaudhury[a] and Timothy Weaver
Department of Chemical Engineering, Lehigh University, Bethlehem, Pennsylvania 18015

C. Y. Hui
Theoretical and Applied Mechanics, Cornell University, Ithaca, New York 14853

E. J. Kramer
Material Science and Engineering, Cornell University, Ithaca, New York 14853

(Received 19 January 1996; accepted for publication 29 March 1996)

Methods are developed to estimate the adhesion and surface free energies of compliant materials from the contact deformations of cylindrical lenses with flat sheets. Some important differences are found between the cylindrical contact studied here and the widely studied geometry of spherical contact. For example, while the pull-off force is completely independent of the elastic constants (K) of the materials for spherical contacts, the pull-off force for cylindrical contact is proportional to $K^{1/3}$. Furthermore, for cylindrical contacts the contact width at separation reaches to a value of 39% of the width (a_0) at zero load, whereas the corresponding value is $0.63a_0$ for spherical contact. The feasibility of using cylindrical contacts to estimate the surface and adhesive energies of polymers was investigated using elastomeric polydimethylsiloxane (PDMS) as a model system. PDMS was used in two ways: (1) unmodified and (2) with its surface hydrolyzed with dilute hydrochloric acid. Significant hysteresis of adhesion was observed with the hydrolyzed PDMS surfaces due to H-bonding interactions, which appeared to depend on normal stress. © *1996 American Institute of Physics.* [S0021-8979(96)07213-1]

I. INTRODUCTION

The contact mechanics method of Johnson, Kendall, and Roberts (JKR)[1] is now widely used to study the adhesive interactions between surfaces.[2–20] In this method, a semispherical object is brought into contact with another flat or a semispherical object under controlled loads. If one of the contacting materials is deformable and if their surfaces are smooth, then deformation occurs in the zone of contact, the magnitude of which depends on the work of adhesion between surfaces and any external loads applied on them. The external load is distributed as compressive stress in the central region of contact and as tensile stress at the contact boundary. The large tensile stress accrued at the contact edge is supported by the adhesion of the surfaces. Mechanical calibration of the contact deformation thus allows determination of the work of adhesion and surface free energies of the elastic solid surfaces.

One feature of the force needed to break the contact between curved bodies is that its dependence on material properties depends sensitively on the detailed geometry of the contacting surfaces. For instance, if the work of adhesion is constant (independent of contact radius), the force needed to pull apart a sphere from another sphere or a flat plate is completely independent of the elastic moduli of both bodies,[1,21] whereas it is inversely proportional to the elastic modulus of the substrate, which is indented by a rigid, conical punch.[22] Likewise, while the adherence force of spheres is directly proportional to the work of adhesion[1,21] (W), the adherence force of a conical punch[22] is proportional to W^2. Apart from these differences, there lies another important difference in the way the surfaces separate from contact when a negative load is applied.

When a curved object is pulled out of another adhering substrate, the contact area does not decrease in a stable fashion to zero at separation. Elastic instability sets in earlier and separation takes place from a finite area of contact. For the contact of spheres,[1,21] this instability occurs at a contact radius ($a_{\min}$) which is 63% of the radius of contact at zero load (a_0). For the contact of a flat, rigid circular punch,[23] there is no such minimum radius—the instability begins from the edge of the original contact—whereas, for a rigid, conical punch,[22] $a_{\min}$ is 56% of a_0. All of the above values of $a_{\min}$ are for separations under fixed loads. Under fixed displacement situations, the $a_{\min}$ values, except for the flat punch, can be considerably lower than those specified above.

In a typical contact mechanics experiment, contact deformation is measured first as a function of increasing load, up to a certain load, and then as a function of decreasing load until instability and pull-off occurs. From these measurements, two values of work of adhesion are obtained. Under ideal situations, these two values are the same. For most situations, however, a finite hysteresis of adhesion persists.[2,3,6–20] A finite adhesion hysteresis for elastic solids indicates that nonequilibrium processes occur at the interface, which is related to the physico–chemical reconstruction of the interfacial structures. Since the interfacial stress is not uniform in the contact zone for curved surfaces, i.e., it is tensile at the edge and becomes progressively more compressive toward the center, it has been stipulated that interfacial reconstruction can at times be sensitive to the spatial variation of the normal stresses.[16] In order to obtain a complete picture of the effect of normal stress on interfacial reconstruction, it is important to drive the separation of the sur-

[a]Author to whom all correspondence should be addressed.

 0021-8979/96/80(1)/30/8/$10.00

faces during unloading, as much as possible, to the center of contact. Because of the limitation imposed by elastic instability, however, separation takes place before the center of contact is reached. Tirrell *et al.*[13] performed experiments with contacting spheres under a fixed displacement condition. In this case, the minimum contact radius that can be achieved is 30% of a_0—much smaller than the fixed load value ($0.63a_0$). The situation can, in principle, be improved using other geometries. For example, under a fixed displacement situation, the contact radius can be driven to 6% of a_0 with a conical punch.[22] The disadvantage with a conical punch however is that the compressive stress at the center of contact is very high[21,22] (theoretically it is infinity), which can cause inelastic deformations of the substrates. We will show here that the contact of a cylinder lying parallel to a flat substrate can be decreased to a value of $0.39a_0$ under fixed load situation, which is lower than the corresponding values for spherical and conical punches. A further advantage of studying contact deformation using cylinders is that they can be rolled on a flat plate, so that the trailing edge traverses the entire area of original contact, thus providing information about the spatial variation of the work of adhesion.

Roberts[24] first reported the experimental results of the contact deformation produced on contacting glass cylinders with rubber slabs under external loads. However, he did not analyze the data to obtain adhesion energies as a result of an analytical difficulty that was experienced with respect to the elastic displacement for this geometry. Instead, Roberts used the rolling of cylinders over flat inclined plates to estimate the magnitude of adhesion hysteresis. The hysteresis of adhesion was estimated from the weight of the cylinder (mg), the angle of inclination (Θ), and the length (l) of the cylinder according to

$$\Delta W = mg \sin \Theta / l. \tag{1}$$

Barquins derived the theory of the contact deformation of cylinders using the method of contact mechanics as pioneered by Greenwood and Johnson[25] and verified it experimentally for steel cylinders indenting rubber sheets. Here, we investigate the utility of the theory to predict the surface and adhesion energies of elastomeric polydimethylsiloxane (PDMS). PDMS was chosen as a model system, because it has been used extensively in the past for several JKR studies, from which some of the material characteristics of the polymer have been well understood.[7–11,16]

The experiments were carried out both with the extracted networks of a commercial elastomer (Dow Corning® Syl-170) and with its surfaces hydrolyzed with dilute hydrochloric acid. The acid-hydrolyzed surfaces form hydrogen bonds across interfaces, which thus increases the adhesion hysteresis. The effect of normal stress on adhesion hysteresis was studied with PDMS using cross cylinders and cylinder–flat plate geometries.

II. MECHANICS OF CONTACT OF A CYLINDER AND A FLAT PLATE

The energy of adhesion was obtained by Barquins[27] for this case of two-dimensional contact of a cylinder and a half-space using a fracture mechanics approach. This fracture mechanics approach was used earlier by Greenwood and Johnson[25] as well as by Maugis *et al.*[26] to solve the problem of spherical contacts. Although the detailed derivation of the required equations can be found in Ref. 27, we briefly reiterate the calculation procedure here for the sake of completeness, as certain arguments developed here will be required for the latter discussions in the article.

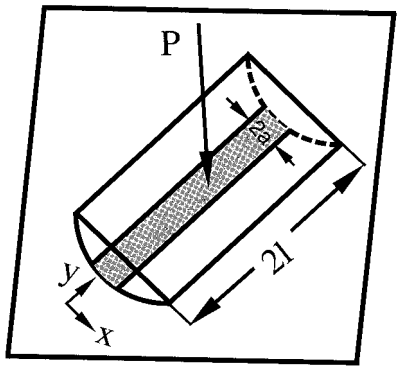

FIG. 1. Schematics of the deformation of contact of a semicylinder lying parallel to a flat substrate.

When two cylindrical bodies with their axes both lying parallel to the y axis are pressed into contact by a force P per unit length in the z direction, the contact zone is a strip of length $2l$ and width $2a$ lying parallel to the y axis (Fig. 1). We define $F = P/2l$ as the force per unit length of cylinder. If we assume $l \gg a$, then the problem reduces to a two-dimensional one, i.e., that of plane strain deformation. Let E_i and ν_i denote the Young's modulus and Poisson's ratio of the cylinders, respectively ($i=1,2$). The normal contact stress $\sigma(x)$ in the contact zone $(-a,a)$ can be found in Ref. 21, i.e.,

$$\sigma(x) = -\{1/[\pi(a^2-x^2)^{1/2}]\}\{F - F_0[(2x^2/a^2)-1]\}, \tag{2}$$

where

$$F_0 = \pi E^* a^2/4R,$$
$$1/E^* = (1-\nu_1^2)/E_1 + (1-\nu_2^2)/E_2, \tag{3}$$
$$1/R = 1/R_1 + 1/R_2.$$

The R_i's are the principal radii of curvature of the cylinders. Here, a positive $\sigma(x)$ denotes a tensile stress. Equation (2) implies that, unless

$$F = F_0 = \pi E^* a^2/4R,$$

the contact stress at the edges $x = \pm a$ has a square root singularity, where F_0 is the Hertzian contact force per unit length. Furthermore, if

$$F < F_0 = \pi E^* a^2/4R,$$

the contact stress is tensile in the region

$$1 > (x/a)^2 > (1/2) + (F/2F_0)$$

of the contact zone. In classical Hertz theory, one requires that $F = F_0$, so that the normal stress in the contact zone is bounded and everywhere compressive. In JKR theory, tensile stresses can be sustained by the presence of adhesive forces,

so that F can be less than F_0. In this case, Eq. (2) implies that the normal stress at $x=\pm a$ has a square root singularity. Indeed, as x approaches a, Eq. (2) implies that

$$\sigma(x)\approx K_1[2\pi(a-x)]^{-1/2}, \tag{4}$$

where

$$K_I=(F_0-F)/(\pi a)^{1/2}. \tag{5}$$

K_I is the stress intensity factor in mode I associated with the crack tips at $x=\pm a$ and is related to the energy release rate G by

$$G=K_I^2/2E^*=(F_0-F)^2/2E^*\pi a. \tag{6}$$

In the JKR theory, G is equated to the adhesion energy W of the two solids. Equation (6) becomes

$$F=\pi E^* a^2/4R-(2E^*\pi a W)^{1/2}. \tag{7}$$

Using the commonly used notation,

$$K=4E^*/3.$$

Equation (6) can also be expressed as

$$W=[(3\pi K a^2 l/8R)-P]^2/(6\pi K a l^2). \tag{8}$$

Equation (8) is the desired equation needed to analyze the adhesive contact deformation of parallel cylinders or a cylinder lying parallel to a flat plate.[28]

Equation (7) can be expressed in a dimensionless form [Eq. (9)] using the following definitions of normalized load (Y) and normalized displacement (X):

$$Y=4F/\pi E^* R,$$

$$X=(a/R)^{1/2}, \tag{9}$$

$$Y=X^4-4\Gamma X,$$

where Γ is a dimensionless parameter,

$$\Gamma=(2W/\pi E^* R)^{1/2}.$$

It is easy to show that the minimum line load $F_{\min}=-3\Gamma^{4/3}\pi E^* R/4$ occurs at $X^3=\Gamma$. From this expression the adherence force is found to be

$$P_{\min}=3.16(KW^2R)^{1/3}l. \tag{10}$$

Note that the relation $Y=X^4$ predicted by classical Hertzian theory is approached by Eq. (9) when $X\gg\Gamma$.

III. EXPERIMENTAL DETAILS

In order to verify Eqs. (9) and (10) experimentally, we employed cylindrical lenses and flat sheets of polydimethylsiloxanes. These results were compared with those obtained with the classical systems of spheres on flat plates. The hemispheres were prepared by curing small drops of the polymer on a perfluorinated glass slide[7] (Fig. 2). The PDMS semicylinders were prepared by polymerizing silicones on perfluoroalkyl silane treated thin glass cover slips (3 mm×60 mm). The liquid polymer is contained within the strip and sets to an elastomer (Fig. 2). The polymer was allowed to cure first at room temperature overnight and then was heated at about 70 °C for 1 h. PDMS flat sheets were prepared in a similar way by pouring the fluid in a polystyrene petri-dish.

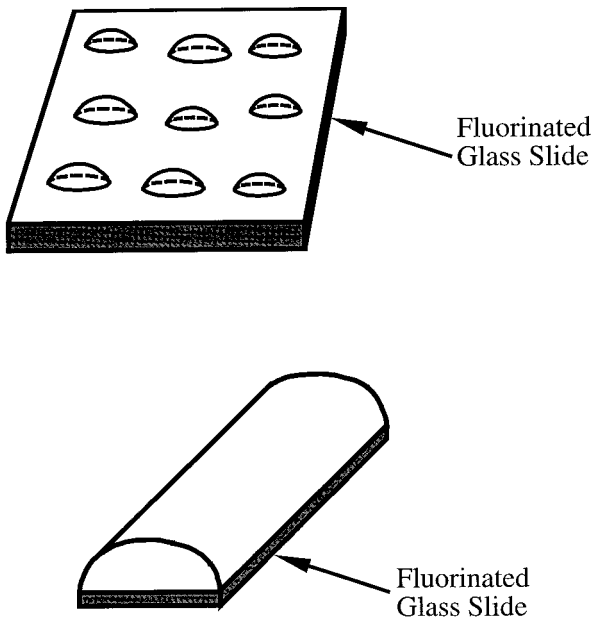

FIG. 2. The method of preparation of PDMS semispheres and semicylinders is shown schematically. The reaction mixture is poured onto perfluorinated glass slides or cover slips (1 mm×3 mm×60 mm), which is confined by the surface tension or the boundary edges of the glass strip. After the polymer is cured, it can be removed from the glass strip.

Followed by polymerization, the PDMS lenses and flat sheets were allowed to swell in chloroform for at least a day by changing the solvent three times. It was found by Silberzan *et al.*[16] that such a treatment removes all the sol fraction from the elastomer. After extraction, the solvent is allowed to evaporate slowly from the swollen polymer; the residual solvent was removed under low vacuum. Two types of PDMS were used for contact deformation experiments: One was chemically unmodified and the other was hydrolyzed partially by treating it with dilute hydrochloric acid. In order to hydrolyze the surface of PDMS, the polymer was immersed in aqueous solution of HCl (pH≈1.7) overnight. The polymer samples were then washed in distilled water dried with nitrogen and held under low vacuum.

Contact deformation experiments were performed using a modification of the method described in Eq. (7). Small pieces (1–1.5 mm long) of the cylinder were cut out by razor blades, and were placed on another flat elastomer substrate or freshly cleaved muscovite mica with its curved side touching the flat sheet (Fig. 1). Before applying external loads, the flat side of the semicylinder was covered with a relatively rigid circular glass plate, which ensures a uniform line load acting in the contact zone of the cylinder and flat plate. The rectangular contact area was viewed through a microscope, and could be recorded in a VCR or printed by a video printer (Fig. 3). Most of the data reported in this article were from the measurements made directly from the video screen. External load was applied by pressing the cylinder against the flat sheet with a semicircular leaf-spring connected to a micromanipulator. The load was recorded using a mettler electrobalance. In some experiments, after the initial contact was made, the load was decreased to a negative value and then

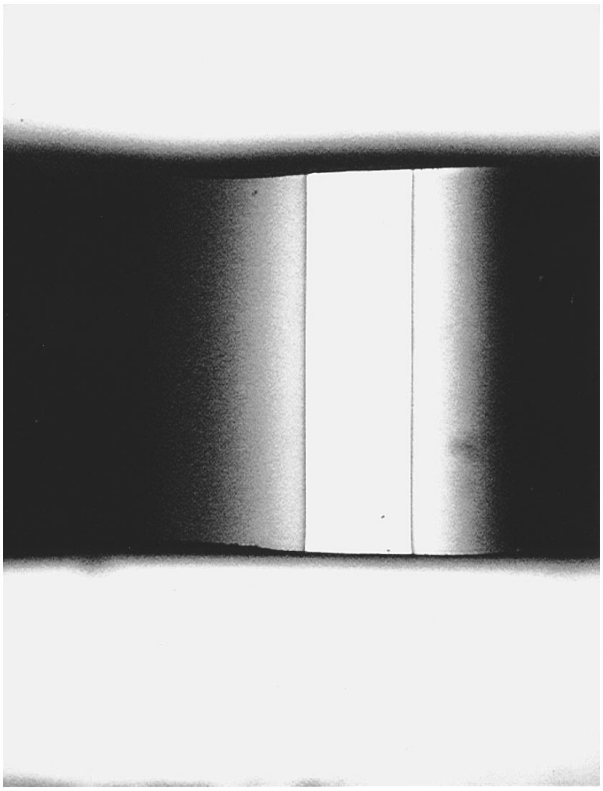

FIG. 3. Typical contact deformation produced on contacting a PDMS semicylinder with a PDMS flat sheet. The contact width here is 0.04 cm.

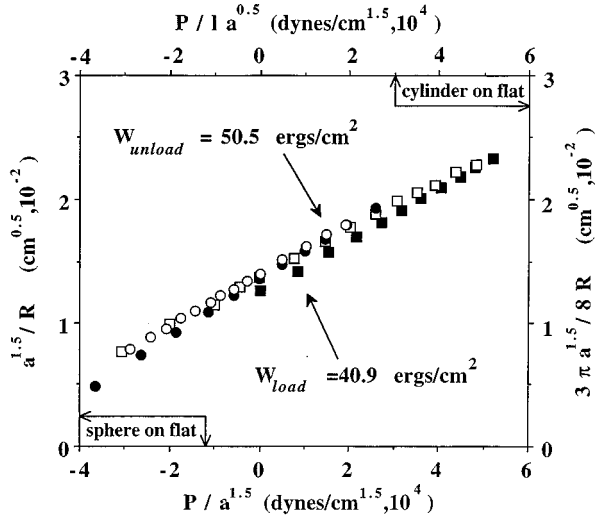

FIG. 4. Normalized plots of contact deformation obtained for spheres and cylinders of PDMS in contact with PDMS flat sheets. The PDMS used here were extracted in chloroform and dried. Note that the functions $P/a^{1.5}$ and $P/la^{0.5}$ have the units of stress intensity factor, K_I. Sphere on flat: ■=loading, □=unloading. Cylinder on flat: ●=loading, ○=unloading. Here, 1 erg/cm^2=1 mJ/m^2 and 1 dyn/cm$^{1.5}$=10^{-2} N/m$^{1.5}$.

the loads were increased by positive increments to a certain maximum value, before the unloading process began. In this method, a large number of data points were available for the estimation of surface and adhesion energies. The experiments were conducted at normal atmospheric conditions. The room humidity was in the range of 35%–40%. The radii of curvatures of the spherical and cylindrical lenses were measured from their sideviews that were observed with a microscope and projected directly on a video screen or printed with a video printer.

IV. RESULTS AND DISCUSSION

A. Experiments with unmodified PDMS

The contact deformations as a function of external loads were analyzed using the following form of Eq. (8):

$$(3\pi/8)a^{3/2}/R=(P/Kla^{1/2})+(6\pi W/K)^{1/2}. \tag{11}$$

A plot of $(3\pi/8)a^{3/2}/R$ vs $P/la^{1/2}$ leads to a straight line, the slope and intercept of which yield the values of modulus and work of adhesion, respectively.

In order to examine the validity of the results obtained from the deformation of the cylinders, we have also performed similar contact deformation experiments with semispherical lenses and flat sheets of PDMS. The experimental data with semispheres were examined graphically by rearranging the classical JKR equation in the following format:

$$a^{3/2}/R=(P/Ka^{3/2})+(6\pi W/K)^{1/2}. \tag{12}$$

In this case, K and W are obtained graphically by plotting $a^{3/2}/R$ vs $P/a^{3/2}$. Since, the intercepts and slopes of the lines obtained from linear plots for the above two cases are the same, the data for the two types of contact can be compared graphically. Figure 4 shows such a plot. The average value of W obtained from the loading and the unloading experiments are about 40 and 50 ergs/cm^2, respectively, showing a small amount of hysteresis. The surface free energy of the polymer ($W/2$) is estimated to be 20–25 ergs/cm^2, which is very close to the value of the surface tension of PDMS.

B. Measurements of pull-off forces

We measured the force necessary to pull-off several PDMS semicylinders ($R\approx$2.3 mm) from PDMS sheet and mica. Some of these results are given below. Because of slight variability of the elastic constant (K) and the work of adhesion (W_{un}) obtained from the unloading experiments, these cases are discussed separately. For a cylinder of l=0.53 mm, the pull-off force from a PDMS sheet was 253 dyn. Substitution of the respective values of K and W_{un} as 4.76×10^6 dyn/cm^2 and 50 ergs/cm^2 in Eq. (10) predicts a pull-off force (235 dyn) for this case. For a longer cylinder (l=0.86 mm), the pull-off force increases to 361 dyn, which compares well with the predicted value of 346 dyn ($K=4.37\times10^6$ dyn/cm^2; W=45.4 dyn/cm). When a PDMS cylinder (l=.6 mm) is pulled off a sheet of mica a pull-off force of 351 dyn was recorded. This increase of the pull-off force is primarily due to the increase of the elastic constant K (9.36×10^6 dyn/cm^2). The high value of K here is due to the fact that mica is nondeformable compared to PDMS and thus the effective value of K (or E^*) is almost double the value of K (or E^*) for PDMS–PDMS contact. The calculated pull force for this case is 322 dyn with W=47.4 dyn/cm. Even

though the discrepancy between the calculated and experimental pull-off forces is less than 10% in all cases, there is a systematic trend to underpredict the pull-off forces somewhat. We have not explored the origin of this discrepancy in detail (because the discrepancy is small), but speculate that it might be due to a slight variation of W with respect to contact width during the unloading process. This point is elaborated in detail in the next section.

C. Experiments with hydrolyzed PDMS

Previously, Silberzan *et al.*[16] observed a high adhesion hysteresis for spherical contacts of PDMS elastomers, when the sol fraction of the polymer was extracted and the polymer was dried in an oven overnight at low vacuum. The authors found that the unloading branch of the load-deformation cycle did not follow the classical JKR behavior. It was proposed that the discrepancy is due to the variation of the hydrogen bonding interaction, an effect produced by the spatial variation of the normal stress. We have reproduced the general features of this earlier observation using PDMS elastomers, whose surfaces were treated with a dilute hydrochloric acid. It is well-known[29] that the aqueous solution of hydrochloric acid hydrolyzes the siloxane bonds and generate silanols, which is consistent with the high adhesion hysteresis observed with hydrolyzed PDMS lenses and flat sheets. We, however, do not know, at present, the concentration of the silanols on the hydrolyzed PDMS surface. However, for the discussions to follow it is not necessary to know the surface concentration of silanols, because the phenomena that we report can be understood on the basis of the overall mass action behavior.[30]

The contact deformation experiments with hydrolyzed PDMS surfaces were carried out in two ways: using a cross cylinder geometry and using a cylinder lying parallel to the surface of a PDMS flat plate. The mechanics of deformation of cross cylinders are identical to those of a sphere on flat plate and thus it is amenable to the same JKR equation that is applicable for spheres. The major advantage of performing the experiments this way is that at least one of the cylinders can be used as a common substrate for both the experiments. The data summarized in Fig. 5 show that all the surfaces exhibit significant adhesion hysteresis. The data obtained from the loading branch fall on a straight line for all surfaces, from which the work of adhesion is estimated to be $\sim 40-45$ dyn/cm^2. Significant curvatures seen with the plots obtained from the unloading experiments indicate a non-JKR behavior, consistent with what was reported by Silberzan *et al.*[16]

The basic idea behind the non-JKR behavior as hypothesized by Silberzan *et al.* is that the interfacial chemical reaction, in this case hydrogen bonding, depends on the normal stress. Since the stress is maximally compressive at the center, the extent of hydrogen bonding is also highest there. The extent of H bonding continues to increase from the edge to the center of contact, where the stress is more compressive. As a result of the stress-induced interfacial H bonding, the work of adhesion becomes position dependent. Thus, when the surfaces are separated during unloading, the work of adhesion continues to increase as the contact area shrinks. If one were to force the data to fit the classical JKR equation,

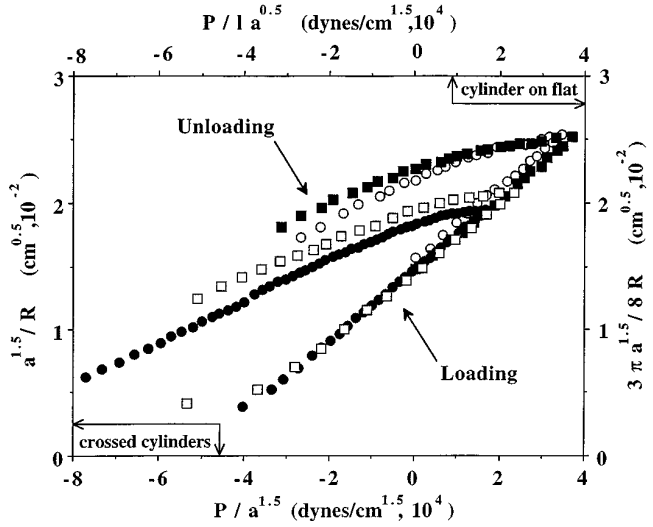

FIG. 5. Normalized plots of contact deformation obtained for PDMS elastomers in the configurations of cross cylinders and cylinders lying parallel on a flat sheet. The polymers used here were hydrolyzed in dilute hydrochloric acid. Note that all the data obtained from the loading experiments fall on a straight line, whereas the data obtained from the unloading show the non-JKR behavior. Both the loading and unloading data are represented using the same symbol. Cylinder on flat: ● and □. Cross Cylinders: ○ and ■. Here, 1 dyn/cm$^{1.5}$=10^{-2} N/m$^{1.5}$.

unrealistic values of elastic moduli or work of adhesion are obtained. A better way to analyze the data is to use the elastic constants obtained from loading experiments in order to estimate W from Eq. (8). Since the interfacial normal stress can also be determined by using Eq. (2), the above method[16] allows us to examine how W varies with normal stress. The distribution of normal stress for spherical and cylindrical contacts were estimated using the following equations:
Sphere on flat surface or cross cylinders:

$$\sigma(x) = -\{1/[2\pi(a^2-x^2)^{1/2}]\} \times [P/a-(K/R)(3x^2-2a^2)]. \tag{13}$$

Cylinder lying parallel to a flat surface:

$$\sigma(x) = -\{1/[2\pi(a^2-x^2)^{1/2}]\} \times [P/l-(3\pi K/8R)(2x^2-a^2)]. \tag{14}$$

The plots of work of adhesion versus normal stress [Eqs. (13) and (14)] are summarized in Fig. 6. For both the geometries examined, W increases systematically as the normal stress becomes progressively more compressive, i.e., as the center of contact is approached.[31] When the work of adhesion is position dependent, Eq. (10) cannot be used here to compute the adhesive pull-off forces. Silberzan *et al.*[16] discussed a similar problem for spherical contact and showed that the gradient of the work of adhesion changes the balance of forces and shifts $a_{\min}$ to a value lower than that expected for uniform W. For finite gradient of W, the condition for elastic instability becomes

$$\partial G/\partial a = \partial W/\partial a. \tag{15}$$

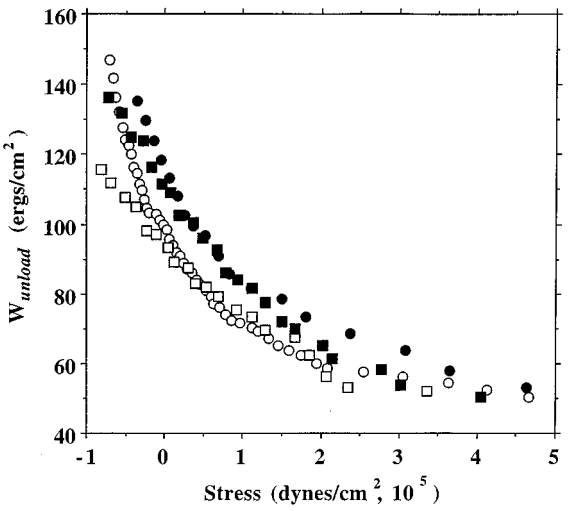

FIG. 6. Plots of work of adhesion (W) vs the normal stress obtained using hydrolyzed PDMS. Both the cross cylinders and cylinder on flat plate show similar trends of W increasing with the increase of normal compressive stress. Cylinders on flat: ○ and ●. Cross cylinders: □ and ■. Here, 1 erg/cm^2=1 mJ/m^2 and 1 dyn/cm^2=0.1 N/m^2.

Using Eqs. (15) and (6), we obtain the value of $a_{\min}$, where elastic instability begins as

$$-(\partial W/\partial a)=(W/a)-(3\pi KaW/8R^2)^{0.5} \quad \text{at } a=a_{\min}. \tag{16}$$

There are two main unknowns in Eq. (16): W and $\partial W/\partial a$. If these two values are computed, the value of $a_{\min}$ can be estimated from Eq. (16) and the pull-off force can be obtained by substituting its value in Eq. (8). An example of this case is given below. Figure 7 shows the typical plot of W_{unload} as a function of contact width for a cylinder (R =0.177 cm and l=0.1026 cm) on a flat plate. The pull-off force in this case is 816 dyn. Close to the pull-off W varies linearly following the relationship: $W=233-9047a$, from which $\partial W/\partial a$ is estimated to be -9047 ergs/cm^3. Substituting these values of W and $\partial W/\partial a$ in Eqs. (16) and (8), we estimate the value of the pull-off force as 798 dyn, which agrees well with the experimentally measured value of 816 dyn.

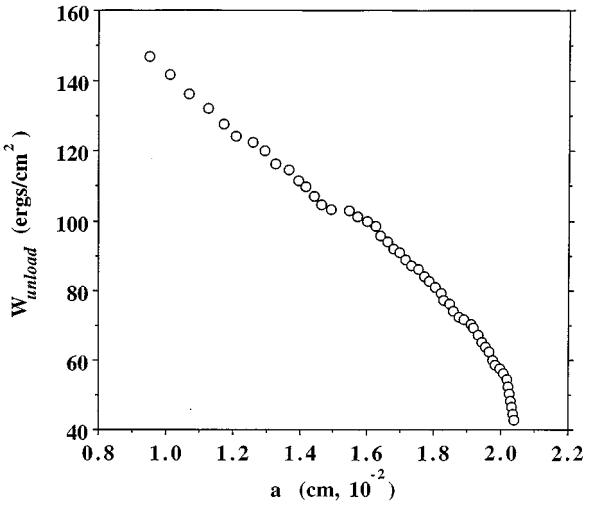

FIG. 7. Typical plot of work of adhesion (W) vs the contact width (a) for hydrolyzed PDMS cylinder on hydrolyzed PDMS flat. Here, 1 erg/cm^2=1 mJ/m^2.

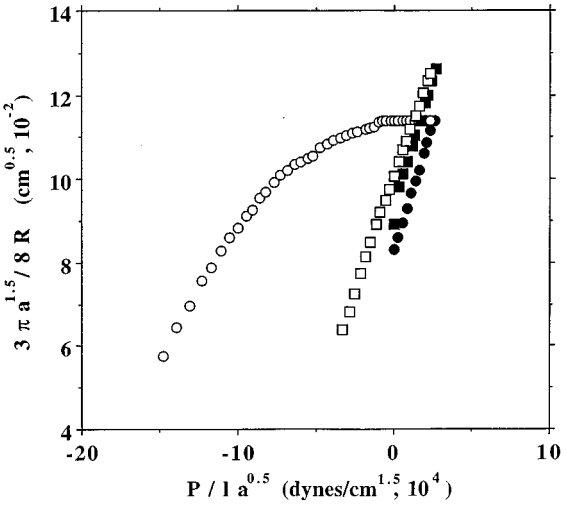

FIG. 8. Normalized plots of contact deformations for elastomeric PDMS cylinders against mica. The unhydrolyzed PDMS exhibits negligible hysteresis, whereas the hysteresis is significant for hydrolyzed PDMS. Although the slopes of the load-deformation data for both cases are similar, indicating that the elastic moduli are the same in both cases, their intercepts on the y axis are different. The unloading data for hydrolyzed PDMS show a non-JKR behavior. Unhydrolyzed PDMS on mica: ■=loading; □=unloading. Hydrolyzed PDMS on mica: ●=loading; ○=unloading. Here, 1 dyn/cm$^{1.5}$ $=10^{-2}$ N/m$^{1.5}$.

In another experiment, load-deformation experiments were conducted with PDMS cylinders against mica. The load-deformation data show negligible adhesion hysteresis for unmodified PDMS against mica; but, a large hysteresis was observed with a hydrolyzed PDMS surface as seen in Fig. 8. The large hysteresis with hydrolyzed PDMS seems to arise from the hydrogen bonding between the oxygen of mica and the silanols of the hydrolyzed polymer.

There is another important detail of these results that deserves some comment. The work of adhesion between hydrolyzed PDMS and mica obtained from the loading experiment is about 30 ergs/cm^2, which is somewhat lower than the value (39 ergs/cm^2) for unhydrolyzed PDMS and mica. There may be two possible explanations for this effect. First, one may hypothesize that some roughness is introduced in the HCl-treated PDMS, thus preventing the polymer to come into intimate molecular contact with mica. However, if that were the case, the work of adhesion for two hydrolyzed PDMS surfaces should similarly be affected by roughness. But, no significant discrepancy between the W_{load} values for hydrolyzed and unhydrolyzed PDMS was observed. The second possibility is that the PDMS–mica interface experiences some amount of friction and thus shear stress develops in response to the uneven deformations of the two components. One cause of uneven deformation is the modulus mismatch of the two components. For PDMS–PDMS interaction, similar shear stress does not arise because both the cylinder and flat plate have identical modulus values, in which case, if a shear stress develops, it should be due to the difference in

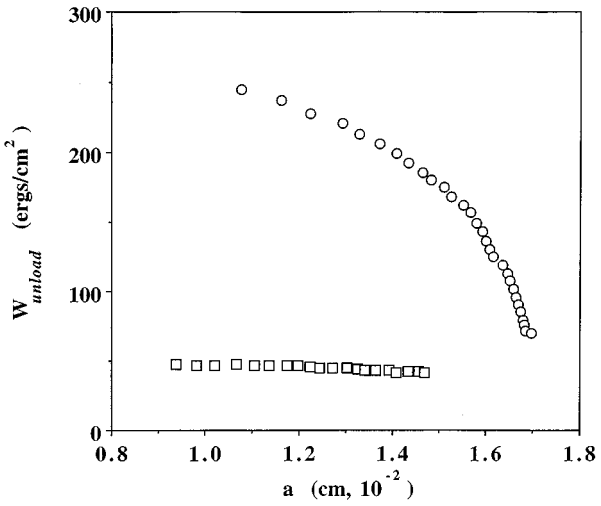

FIG. 9. The data of Fig. 8 is used to construct the plot of W_{unload} vs a. The unhydrolyzed PDMS shows negligible dependence of W on a, whereas W_{unload} increases for hydrolyzed PDMS as the center of contact is approached. Unhydrolyzed PDMS on mica=□; hydrolyzed PDMS on mica=○. Here, 1 erg/cm^2=1 mJ/m^2.

their geometries. If a static friction operates at the interface, its value should be significant for hydrolyzed PDMS and mica, because hydrogen bonding can occur between the two; but its value should be insignificant for unhydrolyzed PDMS and mica. The effect of the friction force is to prevent the contact line to move primarily during the unloading process thus increasing the effective values of W_{unload}. The effect of friction during the loading process should be small but not negligible. Within the current set of experimental results it is not possible to opt for either friction or roughness as the possible source of discrepancy observed in the case of PDMS and mica.

The work of unloading for the cases of hydrolyzed and unhydrolyzed PDMS was determined as a function of the contact width (a) and the results are shown in Fig. 9. W_{unload} remains almost independent of the contact width for unhydrolyzed PDMS, but it increases systematically for the hydrolyzed PDMS as the contact area decreases. Close to the pull-off, W_{unload} varies with the contact width according to the following relationship: $W=382-12709a$. $\partial W/\partial a$ for this system is $-12\,709$ ergs/cm^3, yielding a value of the pull-off force in Eqs. (16) and (8) of 926 dyn, which again agrees well with the value (917 dyn) observed experimentally.

V. SUMMARY AND CONCLUSIONS

Experimental protocols were developed to estimate the adhesive energies of compliant materials using the contact of cylinder and a flat plate. The experimental contact deformations conform well with the theoretical prediction of Barquin. The adhesion results obtained with cylindrical contact are consistent with those derived from the contact of spheres. Experiments with hydrolyzed PDMS support the previous finding that the formation of hydrogen bonds across an interface is dependent on normal stress, and it increases toward the center of contact. This spatial gradient of the work of adhesion affects the balance of forces at elastic instability, increasing the adherence (pull-off) force from the value expected for uniform work of adhesion. The general characteristic pattern observed for cylindrical contact is similar to that of spherical contact, except that the contact width at separation reaches a much lower value than that for spherical contacts. The main disadvantage with the cylindrical contact is that the contact is conformal along the long axis and thus extra care needs to be taken to properly align the cylinders with respect to the flat surface.

ACKNOWLEDGMENTS

This work was supported by a grant from Dow Corning Corporation. C.-Y.H. received support from the NSF-DMR-MRSEC program through Cornell Materials Science Center and E.J.K. from the Office of Naval Research.

[1] K. L. Johnson, K. Kendall, and A. D. Roberts, Proc. R. Soc. London, Ser. A **324**, 301 (1971).
[2] K. Kendall, J. Phys. D: Appl. Phys. **5**, 1782 (1973); **8**, 1449 (1973); Proc. R. Soc. London, Ser. A **341**, 409 (1975); **344**, 287 (1975); J. Adhes. **7**, 137 (1975); J. Mater. Sci. **11**, 638 (1976); **10**, 1011 (1975).
[3] A. D. Roberts and A. B. Othman, Wear **42**, 119 (1977).
[4] D. Tabor, J. Colloid Interface Sci. **58**, 2 (1977).
[5] A. E. Lee, J. Colloid Interface Sci. **64**, 577 (1978).
[6] R. G. Horn, J. N. Israelachvili and F. Pribac, J. Colloid Interface Sci. **115**, 480 (1987).
[7] M. K. Chaudhury and G. M. Whitesides, Langmuir **7**, 1013 (1991).
[8] M. K. Chaudhury and M. J. Owen, J. Phys. Chem. **97**, 5722 (1993).
[9] M. K. Chaudhury and G. M. Whitesides, Science **255**, 1230 (1992).
[10] M. K. Chaudhury, J. Adhes. Sci. Technol. **7**, 669 (1993).
[11] H. Haidara, M. K. Chaudhury, and M. J. Owen, J. Phys. Chem. (in press).
[12] V. Mangipudi, M. Tirrell, and A. V. Pocius, J. Adhes. Sci. Technol. **8**, 1251 (1994); W. W. Merrill, A. V. Pocius, B. Thakkar, and M. Tirrell, Langmuir **7**, 1975 (1991).
[13] M. Deruelle, L. Leger, and M. Tirrell, Macromolecules **28**, 1995 (1995).
[14] K. Kendall, J. Adhes. **5**, 179 (1973).
[15] Y. L. Chen, C. A. Helm, and J. N. Israelachvili, J. Phys. Chem. **95**, 10737 (1991).
[16] P. Silberzan, S. Perutz, E. J. Kramer, and M. K. Chaudhury, Langmuir **10**, 2466 (1994).
[17] M. E. R. Shanahan and J. Michel, Int. J. Adhes. **11**, 170 (1991); see also M. F. Vallat, P. Ziegler, P. Vondracek, and J. Schultz, J. Adhes. **35**, 95 (1991).
[18] D. S. Rimai, L. P. DeMejo, and R. C. Bowen, J. Appl. Phys. **68**, 6234 (1990); R. C. Bowen, D. S. Rimai, and L. P. DeMejo, J. Adhes. Sci. Technol. **3**, 623 (1989); L. P. DeMejo, D. S. Rimai, and R. C. Bowen, *ibid*. **2**, 331 (1988); **5**, 959 (1991).
[19] K. Kendall, Wear **33**, 351 (1975).
[20] M. K. Chaudhury and M. J. Owen, Langmuir **9**, 29 (1993).
[21] K. L. Johnson, *Contact Mechanics* (Cambridge University Press, Cambridge, 1985).
[22] D. Maugis and M. Barquins, J. Phys. Lett. **42**, L95 (1981).
[23] K. Kendall, J. Phys. D: Appl. Phys. **4**, 1186 (1971).
[24] A. D. Roberts, Rubber Chem. Technol. **52**, 23 (1979).
[25] J. A. Greenwood and K. L. Johnson, Philos. Mag. **43**, 697 (1981); D. Maugis and M. Barquins, J. Appl. Phys. D **11**, 1989 (1978).
[26] D. Maugis and M. Barquins, *Adhesion and Adsorption of Polymers: Polymer Science and Technology*, edited by L. H. Lee (Plenum, New York, 1980), Vol. 12A, p. 203; M. Barquins and R. Courtel, Wear **32**, 133 (1975).
[27] M. J. Barquins, Adhesion **26**, 1 (1988).
[28] In a recent personal communication with K. L. Johnson (1994) M.K.C. learned that Professor Johnson independently derived Eq. (8) to analyze some data of the rolling friction measurements.
[29] A. G. Martollock, International Conference on Elastoplastic Technology, Wayne State University, 24 March, 1966 (unpublished); W. J. Bobear, Rubber Age **84**, 448 (1958); A. H. Horner, *Division of Polymer Chemistry* (American Chemical Society, Boston, 1959).

[30] In a separate study, we found that the formation of interfacial hydrogen bonds follows roughly a second-order kinetics indicating a bimolecular reaction at the interface, from which we estimated the product of the concentration of the surface silanol and the second-order rate constant as 5.2×10^{-3} min^{-1}.

[31] When we performed similar experiments with spherical lenses ($R=1.2$ mm), the W vs $\sigma(x)$ plots lay slightly lower than the plots shown in Fig. 6. We believe the reason for this discrepancy is due to a combined effect of stress and contact time, which are different in these cases because of the differences in the radii of curvatures of the spherical lens and the cylinders (2 mm) used. However, when the sphere was allowed to make contact with the cylinder for a slightly longer period of time ($\sim$10 min), the discrepancy became small.